Journal of Materials Chemistry B

RSC Publishing

PAPER

View Article Online
View Journal | View Issue

Cite this: J. Mater. Chem. B, 2013, 1, 6283

A new method for the preparation of biocompatible silica coated-collagen hydrogels

Maria Lucia Foglia,*[a] Daniela Edhit Camporotondi,[a] Gisela Solange Alvarez,[a] Sascha Heinemann,[b] Thomas Hanke,[b] Claudio Javier Perez,[c] Luis Eduardo Diaz[a] and Martin Federico Desimone*[a]

Received 1st August 2013
Accepted 22nd September 2013

DOI: 10.1039/c3tb21067g

www.rsc.org/MaterialsB

Silica–collagen scaffolds were obtained by covalent binding of an aminosilane to glutaraldehyde fixed collagen hydrogels, rendering a three dimensional network of silicon coated collagen fibrils. When compared to non-silicified collagen, silica containing matrices exhibited a 60 fold increment in the rheological properties. Moreover, acellular degradation by collagenase type I indicated that enzymatic digestion occurred at a slower rate for silica modified hydrogels, hence enabling a controlled degradation of the obtained material. In addition, fibroblastic cells seeded on silicified collagen matrices were able to adhere, proliferate and migrate within the scaffold for over 3 weeks as shown by MTT tests and hematoxylin–eosin staining. These results suggest that the herein described method could be useful in the design of materials for tissue engineering purposes.

1. Introduction

The interest in new biomaterials has risen during the past years due to the necessity to fill tissue loss areas caused by trauma or surgical extraction. In the field of tissue engineering, one of the main challenges is to design materials with improved mechanical and biocompatible properties capable of promoting tissue regeneration and/or wound healing.[1] Currently, research involving a combination of molecular biology and mechanical engineering focuses on the interaction between stromal cells and biopolymer interfaces.[2]

For this purpose, a number of biodegradable and bioresorbable materials, as well as scaffold designs, have been experimentally and/or clinically studied. Ideally, a scaffold should present the following characteristics: (i) a three-dimensional and highly porous interconnected network for cell growth and transport of nutrients and metabolic products; (ii) must be biocompatible and bioresorbable with controllable degradation and resorption rates to match cell/tissue growth *in vitro* and/or *in vivo*; (iii) a suitable surface chemistry for cell attachment, proliferation, and differentiation and (iv) mechanical properties to match those of the tissue at the site of implantation.[3]

Hence, a variety of synthetic and naturally derived materials could be potentially used to form hydrogels suitable for tissue engineering applications. Synthetic materials include poly(ethylene oxide) (PEO), poly(vinyl alcohol) (PVA), poly(acrylic acid) (PAA), poly(propylene fumarate-*co*-ethylene glycol) (P(PF-*co*-EG)), and polypeptides. Representative naturally derived polymers include agarose, alginate, chitosan, collagen, fibrin, gelatin, and hyaluronic acid (HA).[4]

Among naturally derived polymers, collagen is attractive for biomedical applications as it is the most abundant protein in mammalian tissues and the main constituent of the extracellular matrix.[5] Therefore, the use of type I collagen in the preparation of materials for medical purposes has been favored because it provides a natural anchoring moiety for attachment and survival of the cells,[6] it is highly biocompatible and can be tailored into highly porous implantable devices. However, its lack of mechanical stability has stimulated its use in combination with other compounds, especially for load bearing applications.[7] As an example, Hong *et al.* mixed polycaprolactone (PCL), type I collagen, and β-tricalcium phosphate resulting in biocompatible microsized porous scaffolds.[8] Similarly, Ahn *et al.* constructed hybrid materials consisting of solid freeform-fabricated PCL and collagen struts with appropriate pore interconnectivity for bone regeneration.[9] Other approaches to increase collagen's mechanical strength include the use of calcium phosphate phases, either alone[10] or mixed with other additives such as silicon.[11]

Silicon has been recently chosen to be used along with collagen rendering hybrids and nanocomposite materials[12]

[a]IQUIMEFA-CONICET Facultad de Farmacia y Bioquímica, Universidad de Buenos Aires, Junín 956 Piso 3°, (1113) Ciudad Autónoma de Buenos Aires, Argentina. E-mail: mlfoglia@ffyb.uba.ar; desimone@ffyb.uba.ar; Fax: +54-1149648254; Tel: +54-1149648254

[b]Max Bergmann Center of Biomaterials and Institute of Materials Science, Technische, Universität Dresden, Budapester Str. 27, D-01069 Dresden, Germany

[c]Institute of Materials Science and Technology (INTEMA), University of Mar del Plata and National Research Council (CONICET), J.B. Justo 4302, 7600 Mar del Plata, Argentina

which could be potentially used in dermal dressings[13] and bone implants.[14–16] Its biocompatibility, stability and the various forms it can take through the application of different synthetic routes have made it the additive of choice for increasing collagen's stability and mechanical strength. Still, several limitations exist in the preparation of such materials as silica precursors at high concentrations interfere with collagen's fibrillogenesis, leading to fast gel formation and, in some cases, could alter normal cell function.[11,17]

The covalent linkage of silica to polymers is a research topic that has awakened interest during the past years as silicon release from the composite could be controlled while enabling an improvement in the mechanical properties of the modified material.[18] Normally, this is attained by means of a coupling reagent. As an example, Mahony *et al.* obtained true silica–gelatin hybrids using GPTMS ((3-glycidoxypropyl)-methyldiethoxysilane) as the coupling agent and TEOS (tetraethylorthosilicate) to increase the inorganic–organic ratio.[19] They demonstrated that the obtained scaffolds were able to promote cell adhesion and growth, while exhibiting a controlled silica release profile. Subsequently, Chen *et al.* fabricated collagen–silica hybrids employing for this purpose either GPTMS with porcine type I acid soluble collagen or GPTMS with fish type I atelocollagen rendering membranes which proved to be compatible for the growth of C2C12 skeletal myoblasts and MC3T3-E1 fibroblasts, respectively.[20,21]

Recently, *in vitro* collagen crosslinking was done physically by UV irradiation, chemically, mainly through the use of aldehydes,[22,23] carbodiimides[24] or 1,3-phenylenediacetic acid[25] and enzymatically with enzymes like lysil oxidase or transglutaminase.[26] However, despite the increase in mechanical strength of the cross-linked matrices, most crosslinking procedures lead to non-fibrillar collagen containing scaffolds. Through silicification of collagen fibrils the natural cell environment would be mimicked, as collagen's natural open pored network would be conserved while increasing its mechanical and structural stability.

In this work, a new method for the covalent linkage of silica to free amino groups in fibrillar collagen is proposed. The fibrillar structure of collagen maximizes the strength and provides with large energy dissipation during deformation, creating a tough and robust material.[27] Through silicification of *in vitro* assembled fibrils, it would be stabilized and the final stiffness of the obtained scaffold would be enhanced.

2. Materials and methods

2.1. Hybrid scaffold synthesis

Collagen type I was purified after being obtained from rat tails and the concentration was estimated by hydroxyproline titration.[28] Briefly, collagen gels were made by mixing a 2.1 mg mL^{-1} acidified collagen suspension with a sodium hydroxide solution to attain a final pH of 7.4 and a final collagen concentration of 1.6 mg mL^{-1}. Shortly after, 0.5 milliliters were dispensed into 24 well plates and put in a 37 °C chamber for gel formation to occur. Secondly, glutaraldehyde was added to the previously obtained gels at different concentrations ranging from 0.05 to 0.2 M and left to react at 4 °C for 1 hour. After exhaustive washing with sterile distilled water, a 0.2 M (3-aminopropyl) triethoxysilane (APTES) solution was added and left at 4 °C for 1 hour for the reaction to occur. Finally, gels were rinsed with sterile distilled water and conditioned with phosphate-buffered saline (PBS) and complete DMEM media in order to reach a physiological pH.

2.2. Hybrid scaffold characterization

The scaffolds were analyzed using a Zeiss Supra 40 microscope for Scanning Electron Microscopy (SEM). For this purpose, samples without cells were washed three times with PBS, fixed with a 2.5% glutaraldehyde in PBS solution for 1 h at 4 °C, freeze dried and subjected to gold sputtering prior to analysis.

For infrared spectroscopy, samples without cells were washed three times with PBS, freeze-dried and stored under vacuum conditions until the analysis was performed using a Perkin Elmer Spectrum 100 with a universal ATR (UATR) accessory.

The elastic or storage modulus, $G'(w)$, and the viscous or loss modulus, $G''(w)$, of the materials under study were obtained in small-amplitude oscillatory shear flow experiments using a rotational rheometer from Anton Paar (MCR-301) provided with a CTD 600 thermo chamber. The tests were performed using parallel plates of 25 mm diameter, a frequency range of 0.1–10 s^{-1}, at room temperature (22 °C). All the tests were performed using small strains to ensure the linearity of the dynamic responses. All the samples were tested in triplicate using different samples. The gap width used was 1300 μm.

Accelerated collagenase degradation of the selected materials was studied in the presence of collagenase type I (Gibco®, 260 U mg^{-1}) using a 15 U mg^{-1} suspension in phosphate buffer solution of pH 7.4. The scaffolds under study were incubated at 37 °C in the presence of the enzyme and samples were collected at specific time intervals, washed with distilled water, centrifuged and weighed after freeze drying ($n = 4$).

The amount of silica in each gel was assessed by measuring the ash content of the corresponding scaffolds through mineralization in a muffle furnace at 550 °C until constant weight was achieved. Finally, samples were cooled in desiccators and weighed soon after reaching room temperature. The final weight of silica containing hydrogels was compared to that of non-silicified collagen scaffolds.

2.3. Cell culture

The L929 cell line (mouse fibroblasts) was grown in adherent culture flasks in DMEM (Sigma) supplemented with 10% heat-inactivated fetal calf serum and 1% penicillin–streptomycin. Cells were kept at 37 °C in a humidified 5% carbon dioxide chamber until confluence was reached. Harvesting was done with a trypsin–EDTA solution following the protocol provided by the manufacturer. Before each use cells were stained with trypan blue and counted in a Neubauer camera.

2.4. Cell proliferation experiments

L929 mouse fibroblastic cells (5×10^4 corresponding to 2.5×10^4 cells per cm^2) in passage 8 were added on top of each gel along with 1 mL of cell culture medium. The medium was changed every 3–4 days.

For proliferation experiments, the medium was removed, replaced with 0.45 mL of fresh media and 0.05 mL of a 5 mg mL^{-1} MTT solution and incubated in a humidified 5% carbon dioxide chamber for 4 h. Following incubation, MTT solution was removed, gels were washed three times with PBS and 1 mL of absolute ethanol was added before leaving to stand for 30 minutes. The absorbance was recorded at 570 nm and readings were converted to cell number with a standard curve. In all cases results are expressed as mean ± SD from triplicate experiments.

Cell containing scaffolds were analyzed using a Zeiss Supra 40 microscope for Scanning Electron Microscopy (SEM). For this purpose, samples were washed three times with PBS and fixed with a 2.5% glutaraldehyde in PBS solution for 1 h at 4 °C, freeze dried and subjected to gold sputtering prior to analysis.

For hematoxylin–eosin staining, samples were washed with PBS, fixed with formalin and embedded in paraffin. Sections, 10 μm thick, transverse to the sample surface, were cut with a manual microtome. Paraffin sections were then rehydrated and stained with hematoxylin–eosin. The sections were finally dehydrated, mounted between the slide and the coverslip, and observed with an optical microscope.

2.5. Statistical analysis

Data are means ± SD. The differences were analyzed using a two-way ANOVA, followed by a Bonferroni multiple comparison test; $p < 0.05$ was considered significant.

3. Results and discussion

3.1. Hybrid material characterization

The purpose of this work was to obtain silica–collagen hybrids through covalent linkage of silica to collagen. Taking advantage of readily available free amino groups in collagen, APTES was linked to the protein *via* glutaraldehyde crosslinking as shown in Fig. 1. This was attained in a stepwise reaction which involved the synthesis of a collagen hydrogel as the initial step, followed by glutaraldehyde crosslinking and finally APTES addition with the resultant formation of a colored Schiff base upon the aminosilane reaction with the previously immobilized aldehyde group.

Olde Damink *et al.* have previously shown that at high glutaraldehyde concentrations and long reaction times pendant glutaraldehyde molecules rather than crosslinks are introduced in the collagen matrix, with an average uptake of 2–3 glutaraldehyde molecules per reacted amino group.[22] Thus, it was hypothesized that the higher the glutaraldehyde concentration, the higher the silica binding to the resultant matrix. Several matrices were prepared by varying concentrations of glutaraldehyde and APTES as can be seen in Fig. 2. In all the cases, the final collagen content of the resulting matrices, as determined by hydroxyproline titration, was 1.6 mg mL^{-1}. As can be observed, those matrices containing the highest glutaraldehyde

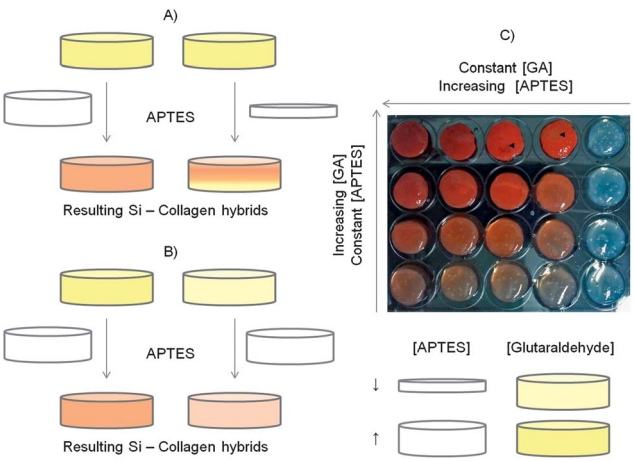

Fig. 2 Experimental setting showing the effect of varying glutaraldehyde and APTES concentrations. (A) Matrices fixed with the same glutaraldehyde concentration (shown in yellow) exposed to different APTES concentrations (shown in white) led to non-homogeneous scaffolds whereas (B) matrices fixed with different glutaraldehyde concentrations (shown in different shades of yellow) exposed to the same APTES concentration (shown in white) led to homogeneous ones. The resulting matrices are shown in (C) with ◄ depicting the non-homogeneous zones.

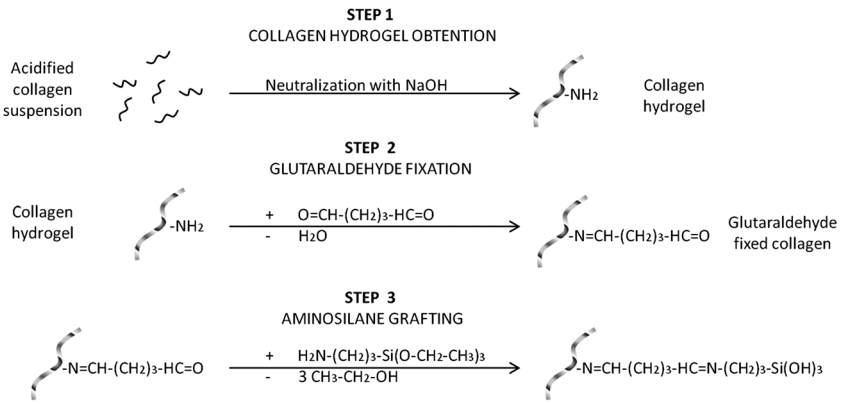

Fig. 1 Overview of the stepwise reaction involved in the obtention of silica-coated collagen hydrogels.

and APTES concentration (0.2 M in both cases) presented a darker coloration probably due to the higher number of carbon–nitrogen double bonds of the Schiff bases formed between glutaraldehyde and the aminosilane. In contrast, gels exposed to glutaraldehyde or APTES alone were transparent indicating that the color came from the interaction between APTES and glutaraldehyde. Taking into account the homogeneity of the resulting scaffolds, the conditions which were found more suitable were those in which a fixed amount of APTES was added to scaffolds containing different amounts of glutaraldehyde. This could be explained as depicted in Fig. 2A and B, considering two facts: firstly, that the reaction depends on the diffusion of the aminosilane through the glutaraldehyde fixed collagen gel and secondly, that once APTES hydrolysis has occurred, it can potentially react either with glutaraldehyde or polymerize through a sol–gel reaction with an already immobilized aminosilane molecule. When glutaraldehyde fixed gels are exposed to decreasing APTES concentrations, gel formation is homogeneous only when APTES availability exceeds the glutaraldehyde content of the gel, otherwise occurs as depicted in Fig. 2A, leading to a non-homogeneous material. On the other hand, when APTES concentration remains constant and glutaraldehyde concentration varies, a homogeneous gel is obtained (Fig. 2B), with the extent of silica grafting being dictated by the amount of glutaraldehyde in the fixed probe. Considering these results, the materials selected for further examination were those prepared by varying glutaraldehyde (0.05–0.2 M) concentrations and adding a fixed amount of APTES (0.2 M) to the previously fixed samples.

Scanning electron microscopy of pure collagen gels showed a classic open pored network formed by thin homogeneous collagen fibrils with a diameter of about 50 nm (Fig. 3A). SEM images of the various silicified collagen matrices (Fig. 3B–D) showed that silica grafting occurred along the previously formed fibrils with conservation of the interfibrillar space. However, the ultrastructure seemed to vary within the different assayed conditions. Particularly, when the lowest glutaraldehyde concentration was employed (0.05 M), separate silica aggregates could be seen along the fibrils (Fig. 3B), whereas more homogeneous coverage was progressively attained by employing higher glutaraldehyde concentrations (Fig. 3C and D). Indeed, the more homogeneously silicified collagen fibrils (obtained with 0.2 M glutaraldehyde and 0.2 M APTES) possessed a diameter of about 100 nm.

IR spectroscopy (Fig. 4) showed the characteristic C=O stretching at 1600–1700 cm^{-1} for amide I and N–H deformation at 1500–1550 cm^{-1} for amide II in both the native and modified collagen matrices, though there was a slight shift to higher wavenumbers as well as an increase in the amide I peak in those samples containing the silane. This could be attributed to the contribution of the C=N bonds formed during covalent linkage of silica to the hybrid scaffolds. Moreover, those samples containing silicon showed the Si–OH stretching band around 1000 cm^{-1} and those containing glutaraldehyde fixed collagen showed characteristic C–H stretching aldehyde bands at ~2900 cm^{-1}, which disappeared in the spectra of silicon containing scaffolds, thus indicating that free pending aldehydic groups have been occupied.

As expected, the silicon content of the scaffolds under study varied with the amount of APTES added as shown in Table 1. Since crosslinks are most likely introduced within fibrils, based

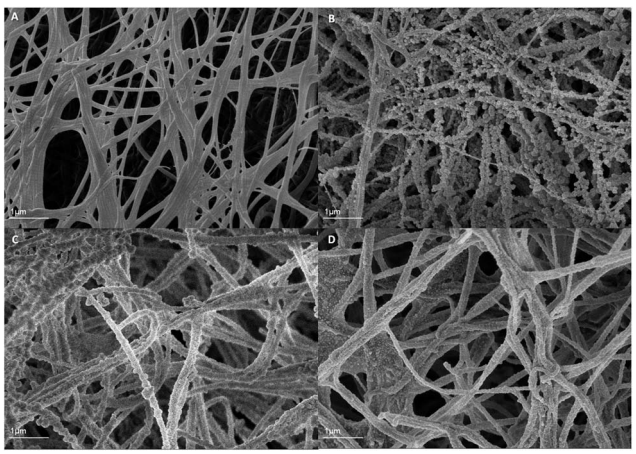

Fig. 3 SEM images showing the microstructure of the different silica-coated collagen materials obtained. (A) Pure collagen hydrogel (B) 0.05 ColGASi (C) 0.1 ColGASi and (D) 0.2 ColGASi.

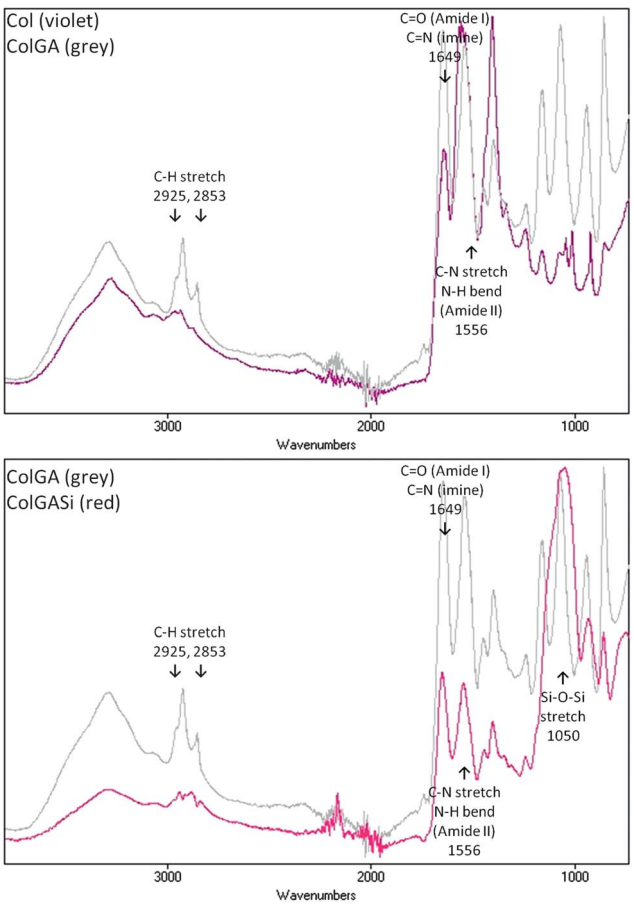

Fig. 4 FT-IR spectroscopy analysis of type I collagen before and after reaction with glutaraldehyde (upper spectra) and glutaraldehyde crosslinked collagen before and after reaction with APTES (lower spectra).

Table 1 Composition of the scaffolds under study

Scaffold	GA (mM)	APTES (mM)	Col (mg mL^{-1})	Si (mg mL^{-1})	%Col–%Si
Col	0	0	1.6	ND	100–0%
0.05 ColGASi	50	200	1.6	0.27 ± 0.04	85–15%
0.1 ColGASi	100	200	1.6	0.51 ± 0.04	75–25%
0.2 ColGASi	200	200	1.6	0.89 ± 0.04	65–35%

on spatial limitations, and given that throughout the experiment conditions such as pH, exposure time, temperature, and APTES and collagen concentrations were maintained constant, the increase in silicon content could be related to an increase in pending aldehyde molecules available for silica grafting. Taking into account that from the available 32–33 mmol of amine groups in collagen, only 26–27 mmol are available for reaction with glutaraldehyde,[22,29] that the amount of silica found in the matrices exceeds this quantity and that the SEM images provided showed silica aggregates covering the fibrils, it is most likely that along with the initial grafting a sol–gel polymerization takes place over the previously fixed aminosilane.

Rheological analysis of all materials under study showed a shear-thinning flow behavior as complex viscosity (η^*) decreased almost linearly with rising frequency indicating structural viscosity. Slopes of the viscosity curves, between −0.75 and −1, indicated that the aqueous collagen systems behave similar to a polymer network with predominantly permanent links (Fig. 5). As shown in Fig. 5a, there is a 10-fold and 60-fold increase in the storage modulus of scaffolds containing the highest amount of silicon (0.2 ColGASi) when compared to glutaraldehyde fixed (0.2 ColGA) and pure collagen gels respectively. Furthermore, when silicon containing matrices were fixed with different glutaraldehyde concentrations (0.05 M–0.2 M) prior to APTES addition, it was observed that the storage modulus increased as well with the increase of silicon content of the matrix under analysis (Fig. 5c), as gels fixed with a 0.05 M glutaraldehyde solution presented an 8-fold

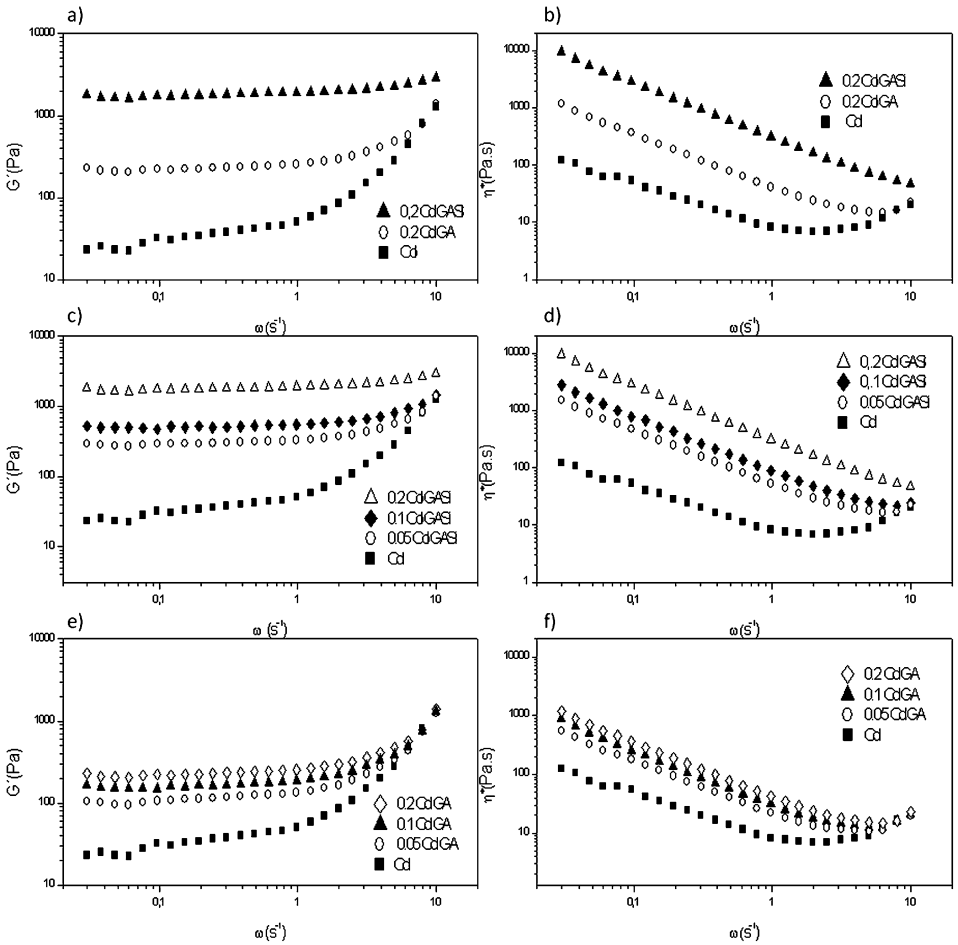

Fig. 5 Frequency dependence of the elastic modulus (G', in Pa) and the complex viscosity (η^*, in Pa s) of all the materials under study at 22 °C. (a) and (b) show the influence of glutaraldehyde fixation and posterior silica grafting for the highest glutaraldehyde concentration (0.2 M), (c and d) the effect of silica content and (e and f) the effect of glutaraldehyde fixation on the rheological properties assayed in comparison with pure collagen scaffolds.

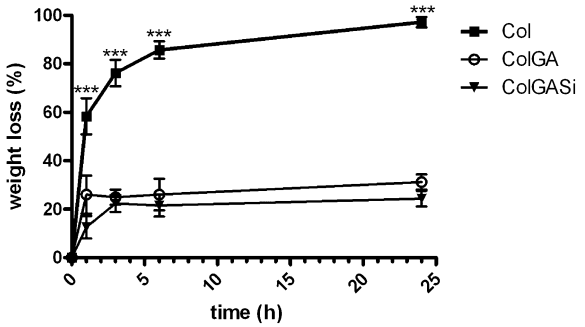

Fig. 6 Accelerated enzymatic degradation of acellular scaffolds by collagenase digestion. Weight percentage loss is shown as a function of time for pure collagen (Col), glutaraldehyde crosslinked (ColGA) collagen and silica-coated collagen hydrogels (ColGASi) data represented as mean (SD, $n = 3$).

increase, whilst those fixed with a 0.2 M solution reached a 60-fold increment in viscosity when compared to pure collagen gels. Finally, the increase of the storage modulus for glutaraldehyde fixed collagen gels is shown in Fig. 3E. As observed, the addition of a small amount of glutaraldehyde (0.05 M) is enough to increase the viscosity to a value about 3 times higher than that of the neat mixture. In addition, as more concentrated aldehyde solutions were employed, the higher the final viscosity obtained, reaching a 6-fold value for the 0.2 M glutaraldehyde condition.

Based on the studied mechanical properties, ultrastructure and inorganic–organic ratios, three matrices were chosen for biocompatibility testing, namely the 1.6 mg mL^{-1} collagen hydrogel (Col), 0.2 M glutaraldehyde fixed collagen (ColGA) and 0.2 M APTES–0.2 M glutaraldehyde collagen (ColGASi).

Collagenase type I degradation of the corresponding matrices showed a significant decrease in the rate of enzymatic digestion for both matrices containing glutaraldehyde when compared to non-fixed collagen gels (Fig. 6). This could be explained as, in order for collagen cleavage to occur, collagenase should gain access to the cleavage site by binding to the enzyme's attachment domains along the α-chains followed by unwinding of the triple helix.[30,31] In this sense, crosslinking through its fixative action could increase the degradation time by blocking the enzyme's access to the cleavage site. These findings are similar to those described by other authors, even when different crosslinking agents were employed.[32]

3.2. Biocompatibility assays

Cell proliferation was studied for 24 days over the selected scaffolds. As can be seen in Fig. 7A, cell growth over silicon containing matrices was comparable to that over plain collagen gels and this was maintained throughout the experiment. As expected, glutaraldehyde containing scaffolds lagged slightly behind, which could be due to the free aldehyde groups being exposed at the material's surface. As growth curves ran parallel, in the case of glutaraldehyde fixed collagen gels, it could be inferred that the initial cell adhesion could have been altered, leading to significantly lower final cell counts.

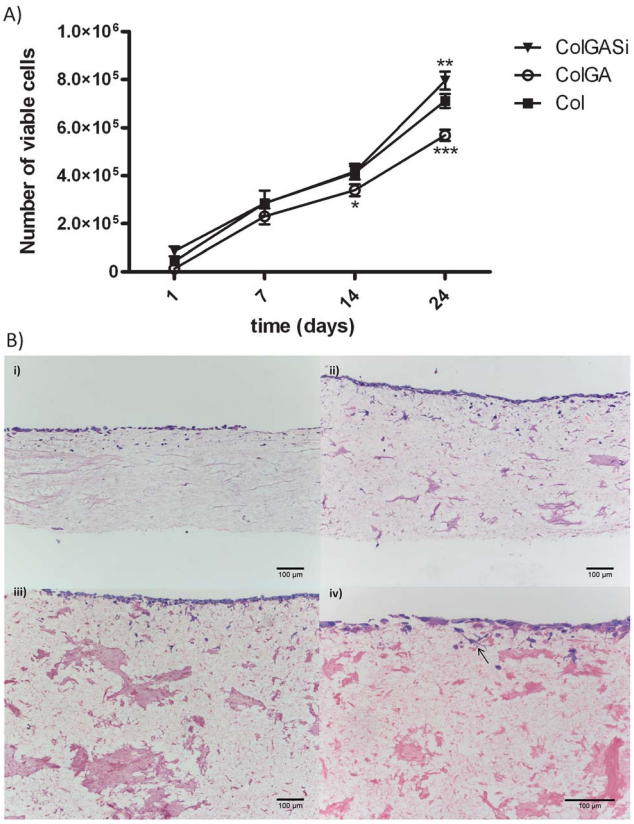

Fig. 7 Proliferation, viability, and penetration of l929 fibroblastic cells within pure, glutaraldehyde crosslinked and silica-coated collagen scaffolds. (A) MTT reduction of the seeded cells when cultured up to 24 days in complete medium over the selected scaffolds ($n = 3$, error bars show SD). * indicates statistically significant differences between silica-coated collagen hydrogels (ColGASi) and glutaraldehyde crosslinked matrices, $p < 0.05$. (B) Hematoxylin–eosin staining of vertical cross-sections show fibroblast's penetration of the materials under study after 24 days. Images are shown for (i) pure collagen, (ii) 0.2 ColGA, and (iii and iv) 0.2 ColGASi. The arrow indicates migrating fibroblasts.

Histological analysis of cell seeded scaffolds after 24 days of cell culture showed cells over the surface and within silica–collagen hydrogels (Fig. 7B). In agreement with acellular collagenase degradation, more cells were able to penetrate pure collagen hydrogels (i) when compared to their fixed collagen counterparts (ii, iii and iv). However, it is interesting to note that material contraction was more evident in pure and glutaraldehyde fixed collagen when compared to the silicified scaffold. It seems that silica coating of collagen fibrils diminishes matrix contraction, thus increasing the surface available for cell attachment and spreading when compared to non-silica containing matrices.

Furthermore, several studies suggest that cell stretching is dependent on the environment's rigidity, as a more rigid matrix would be able to support a more tensioned cytoskeleton.[33–35] In this sense, cell morphology over pure collagen (lowest $G^{\cdot}$ measured) and 0.2 M ColGASi (highest $G^{\cdot}$ measured) was investigated. Scanning microscopy images of cells seeded on top of plain collagen and silicon containing scaffolds showed differential spreading of cells over the matrices. As can be seen in Fig. 8 cells over collagen presented overall a more round

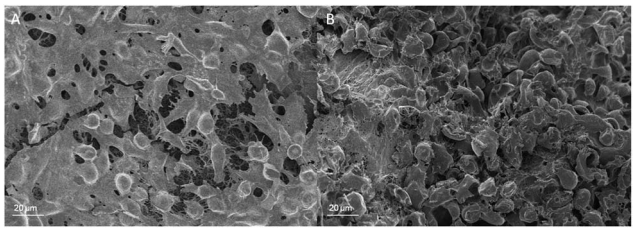

Fig. 8 SEM image showing the influence of the scaffold's structure on cell adhesion after 24 days of cell culture. (A) Fibroblasts over 0.2 ColGASi and (B) fibroblasts over pure collagen gels.

morphology whereas the silicified material's rigidity seemed to stimulate cell stretching leading to an evident cell sheet formation over its surface (Fig. 8B and A respectively).

4. Conclusion

Among the available organic polymers present in nature, collagen offers several advantages, as it is a natural constituent of the extracellular matrix of tissues like skin, bone and cartilage. Since the popularization of relatively easy extraction techniques,[36,37] collagen scaffolds have found a wide variety of applications ranging from *in vitro* culture purposes, such as Optimaix®, to commercially available wound healing inserts such as Biopad®, PuraCol® and Colactive®.

It is well known that, when prepared without additives, diluted collagen hydrogels present poor mechanical properties limiting their use in tissue engineering. Hence, collagen's structural properties need to be enhanced with the aid of crosslinking agents, or additives such as silicon or calcium phosphate phases. Aldehydes have been widely used as crosslinkers for scaffold construction. As an example, Sheu *et al.* have grown fibroblasts over 10 mg mL^{-1} collagen modified with different glutaraldehyde concentrations. They found that the elastic modulus of the resultant matrices increased with the glutaraldehyde content, in close relation to the degree of crosslinking of the resultant matrices.[38] Furthermore, commercially available aldehyde-crosslinked collagen dermal grafts like EZ DERM™ act as a temporary protective barrier, allowing the natural healing process to continue undisturbed.

When considering silica reinforced collagen hydrogels, these have been obtained by mixing either silica precursors like sodium silicate or silica nanoparticles with an acid solubilised collagen type I mixture.[39–41] Upon neutralization with a diluted sodium hydroxide solution, tropocollagen molecules self-assemble into long fibrils with the obtention of a silica–collagen hybrid or nanocomposite material. So far, biocompatible collagen–silica hybrids containing 5 mg mL^{-1} collagen and 25 mM silicate have shown a 10 fold increase in the storage modulus when compared to pure 5 mg mL^{-1} collagen hydrogels (~100 Pa).[41]

In this work, silica grafted collagen gels were prepared, which conserved the fibrillar network of pure collagen hydrogels and presented enhanced mechanical properties. Through the method described here low collagen concentrations are enough to increase the elastic modulus of the material to that of more concentrated collagen gels combining the advantages of stiffness and an open pore structure for the improvement of cell adhesion and proliferation respectively.

Acknowledgements

María Lucia Foglia is grateful for the doctoral fellowship granted by the National Research Council (CONICET). The authors would like to acknowledge the support of grants from the University of Buenos Aires UBACYT 20020110100081 (to M.F.D) and from Agencia Nacional de Investigaciones Científicas y Técnicas PICT 2012-1441 (to M.F.D).

References

1 L. G. Griffith and G. Naughton, *Science*, 2002, **295**, 1009–1014.
2 M. Okamoto and B. John, *Prog. Polym. Sci.*, 2013, **38**, 1487–1503.
3 D. W. Hutmacher, *Biomaterials*, 2000, **21**, 2529–2543.
4 J. L. Drury and D. J. Mooney, *Biomaterials*, 2003, **24**, 4337–4351.
5 C. H. Lee, A. Singla and Y. Lee, *Int. J. Pharm.*, 2001, **221**, 1–22.
6 J. Jokinen, E. Dadu, P. Nykvist, J. Kapyla, D. J. White, J. Ivaska, P. Vehvilainen, H. Reunanen, H. Larjava, L. Hakkinen and J. Heino, *J. Biol. Chem.*, 2004, **279**, 31956–31963.
7 A. M. Ferreira, P. Gentile, V. Chiono and G. Ciardelli, *Acta Biomater.*, 2012, **8**, 3191–3200.
8 S. Hong, M. Kim and G. Kim, *J. Mater. Chem.*, 2012, **22**, 22565–22574.
9 S. Ahn, Y. Kim, H. Lee and G. Kim, *J. Mater. Chem.*, 2012, **22**, 15901–15909.
10 M. Keeney, J. J. J. P. van den Beucken, P. M. van der Kraan, J. A. Jansen and A. Pandit, *Biomaterials*, 2010, **31**, 2893–2902.
11 S. Heinemann, T. Coradin, H. Worch, H. P. Wiesmann and T. Hanke, *Compos. Sci. Technol.*, 2011, **71**, 1873–1880.
12 S. Heinemann, T. Coradin and M. F. Desimone, *Biomater. Sci.*, 2013, **1**, 688–702.
13 I. Jones, L. Currie and R. Martin, *Br. J. Plast. Surg.*, 2002, **55**, 185–193.
14 S. Heinemann, C. Heinemann, R. Bernhardt, A. Reinstorf, B. Nies, M. Meyer, H. Worch and T. Hanke, *Acta Biomater.*, 2009, **5**, 1979–1990.
15 S. Heinemann, C. Heinemann, M. Jäger, J. Neunzehn, H. P. Wiesmann and T. Hanke, *ACS Appl. Mater. Interfaces*, 2011, **3**, 4323–4331.
16 E.-J. Lee, S.-H. Jun, H.-E. Kim and Y.-H. Koh, *J. Biomed. Mater. Res., Part A*, 2012, **100**, 841–847.
17 M. Blondeau and T. Coradin, *J. Mater. Chem.*, 2012, **22**, 22335–22343.
18 J. R. Jones, *Acta Biomater.*, 2013, **9**, 4457–4486.
19 O. Mahony, O. Tsigkou, C. Ionescu, C. Minelli, L. Ling, R. Hanly, M. E. Smith, M. M. Stevens and J. R. Jones, *Adv. Funct. Mater.*, 2010, **20**, 3835–3845.
20 S. Chen, S. Chinnathambi, X. Shi, A. Osaka, Y. Zhu and N. Hanagata, *J. Mater. Chem.*, 2012, **22**, 21885–21892.

21 S. Chen, A. Osaka, T. Ikoma, H. Morita, J. Li, M. Takeguchi and N. Hanagata, *J. Mater. Chem.*, 2011, **21**, 10942–10948.
22 L. H. H. Olde Damink, P. J. Dijkstra, M. J. A. Luyn, P. B. Wachem, P. Nieuwenhuis and J. Feijen, *J. Mater. Sci.: Mater. Med.*, 1995, **6**, 460–472.
23 M. Kikuchi, H. N. Matsumoto, T. Yamada, Y. Koyama, K. Takakuda and J. Tanaka, *Biomaterials*, 2004, **25**, 63–69.
24 H. M. Powell and S. T. Boyce, *Biomaterials*, 2007, **28**, 1084–1092.
25 G. Tronci, A. Doyle, S. Russell and D. Wood, *J. Mater. Chem. B*, 2013, **1**, 5478–5488.
26 R. Parenteau-Bareil, R. Gauvin and F. Berthod, *Materials*, 2010, **3**, 1863–1887.
27 M. J. Buehler, *Proc. Natl. Acad. Sci. U. S. A.*, 2006, **103**, 12285–12290.
28 I. Bergman and R. Loxley, *Anal. Chem.*, 1963, **35**, 1961–1965.
29 J. H. Bowes and C. W. Cater, *Biochim. Biophys. Acta, Protein Struct.*, 1968, **168**, 341–352.
30 C. Overall, *Mol. Biotechnol.*, 2002, **22**, 51–86.
31 P. S. Nerenberg and C. M. Stultz, *J. Mol. Biol.*, 2008, **382**, 246–256.
32 E. Spoerl, G. Wollensak and T. Seiler, *Curr. Eye Res.*, 2004, **29**, 35–40.
33 A. J. Engler, M. A. Griffin, S. Sen, C. G. Bönnemann, H. L. Sweeney and D. E. Discher, *J. Cell Biol.*, 2004, **166**, 877–887.
34 T. Yeung, P. C. Georges, L. A. Flanagan, B. Marg, M. Ortiz, M. Funaki, N. Zahir, W. Ming, V. Weaver and P. A. Janmey, *Cell Motil. Cytoskeleton*, 2005, **60**, 24–34.
35 R. A. Brown, J. B. Phillips and W. J. Kwang, in *International Review of Cytology*, Academic Press, 2007, pp. 75–150.
36 S. Cliche, J. Amiot, C. Avezard and C. Gariepy, *Poult. Sci.*, 2003, **82**, 503–509.
37 N. Rajan, J. Habermehl, M.-F. Cote, C. J. Doillon and D. Mantovani, *Nat. Protoc.*, 2007, **1**, 2753–2758.
38 M.-T. Sheu, J.-C. Huang, G.-C. Yeh and H.-O. Ho, *Biomaterials*, 2001, **22**, 1713–1719.
39 M. F. Desimone, C. Helary, S. Quignard, I. B. Rietveld, I. Bataille, G. J. Copello, G. Mosser, M.-M. Giraud-Guille, J. Livage, A. Meddahi-Pelle and T. Coradin, *ACS Appl. Mater. Interfaces*, 2011, **3**, 3831–3838.
40 M. F. Desimone, C. Helary, G. Mosser, M.-M. Giraud-Guille, J. Livage and T. Coradin, *J. Mater. Chem.*, 2010, **20**, 666–668.
41 S. Quignard, G. J. Copello, C. Aimé, I. Bataille, C. Hélary, M. F. Desimone and T. Coradin, *Adv. Eng. Mater.*, 2011, **14**, B51–B55.

